The electronic transmittance and density of states in triangular quantum well and barrier structures

1996 J. Phys.: Condens. Matter 8 7733

(http://iopscience.iop.org/0953-8984/8/41/018)

J. Phys.: Condens. Matter **8** (1996) 7733–7743. Printed in the UK

The electronic transmittance and density of states in triangular quantum well and barrier structures

A Aldea†, S Vlaev‡, G Monsivais§, F García-Moliner‖ and V R Velasco¶

† Institute of Atomic Physics, PO Box MG 7, Bucharest-Magurele, Romania
‡ Institute of General and Inorganic Chemistry, Bulgarian Academy of Sciences, Sofia 1113, Bulgaria
§ Instituto de Física, UNAM, Apartado Postal 20-264, 01000 México DF, Mexico
‖ Universitat 'Jaume I', Campus Carretera de Borriol, 12080 Castellón de la Plana, Spain
¶ Instituto de Ciencia de Materiales, Consejo Superior de Investigaciones Científicas, Cantoblanco, 28049 Madrid, Spain

Received 18 June 1996

Abstract. A detailed study of the electronic properties of analogue quantum wells and barriers and their supposedly 'equivalent' digital structures is presented. The calculations, based on an sp^3s^* tight-binding model, show that there are significant differences. The digital structures have some diffractive character and this produces a tendency towards some quantum mechanical interference effects which determine some distinctive features in the transmittance and spatial localization at some energies or in some energy ranges. Selected cases are studied in detail showing the differences between analogue and digital structures.

1. Introduction

Heterostructures of the well or barrier type in which the well or barrier region has a variable composition have been extensively studied mostly experimentally [1–12], the interest being stimulated by their potential for device application [3]. In the so-called analogue structures [8–10] the composition varies gradually so one has, say, a triangular profile [1–7] or one with any other shape, while in the structures denoted as digital [8, 11, 12] only two constituent materials, corresponding to two fixed compositions, are employed and their thicknesses change along the well or barrier region according to some chosen algorithm. Figure 1 shows the analogue triangular well and barrier and their corresponding digital structures. Consider, for instance, the analogue well (a). It is clear from inspection that the digital well (b) is also more attractive towards the right and, with a suitable choice of the algorithm, it can be designed to be 'equivalent' to (a). Likewise, the digital barrier structure (d) can be designed to be the 'equivalent' of the analogue barrier (c). Just how equivalent analogue and digital structures are is a query that has sometimes been raised and although some aspects of this question have been discussed, the point of this article is that there are still some significant issues which require further elucidation.

Theoretical studies of these structures are comparatively less abundant and largely based on the use of very simple effective-mass models for the calculation of bound-state energy eigenvalues [1–6], mostly low-lying states. A few more elaborate tight-binding calculations have been reported for electronic states [13–17] and, with some approximations, for the transmittance across the structure [18]. One of these studies [17] showed that in the

0953-8984/96/417733+11$19.50

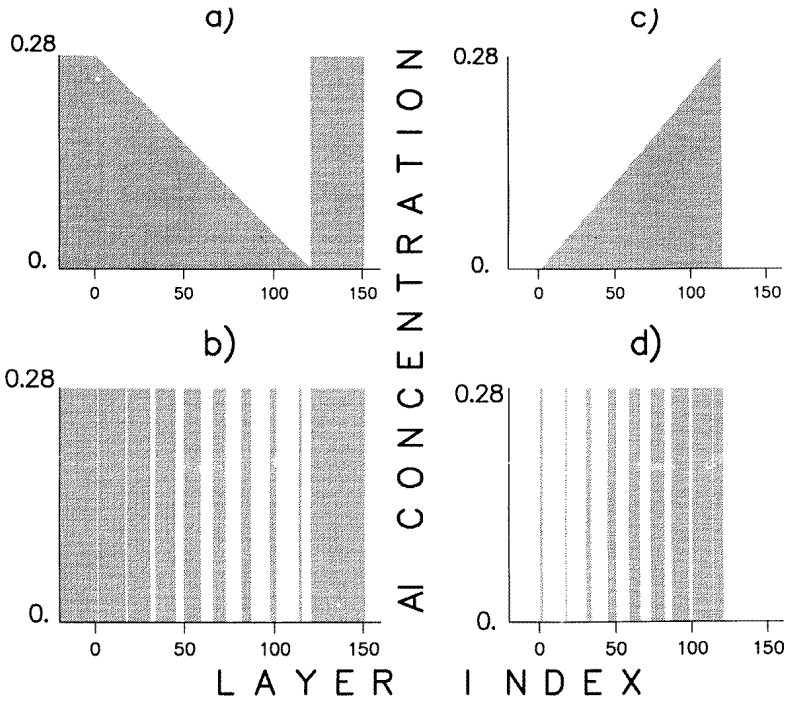

Figure 1. Composition profiles of the four structures studied here. (a) An analogue well. (b) An 'equivalent' digital well; reference [1]. (c) An analogue barrier. (d) An 'equivalent' digital barrier.

triangular well structures of reference [1] one should expect significant differences for higher bound states depending on the growth method (i.e., analogue or digital).

In this article the focus is on the range of propagating states, where a simple effective-mass analysis indicates [19, 20] that one may expect resonances with the continuum producing quasibound states, with amplitude spatially accumulated in the well region. Such states have been observed [21, 22] in some heterostructures. Indeed, the minibands and minigaps in superlattices can be viewed [23] as the result of the interaction between the virtual states of the successive wells. Under some conditions, due to quantum interference effects localized bound states can be formed above the barriers of well [24] or barrier [25] structures.

These then have interesting properties of the type of Bragg reflectors [24–26] and can behave as Fabry–Perot electron filters [27] for incident energies above the barriers. Interference may cause the transmission to vanish and then the wavefunction amplitude is trapped in a bound state of the structure. Depending on the details of the sample this may result in a resonance with the continuum of propagating states; then the incident electron is trapped only temporarily and one finds a *transmission resonance* [28]. These effects have been demonstrated experimentally by various optical techniques like absorption, photoluminescence and reflectivity [19, 21, 23, 27, 28]. These effects have been so far discussed essentially on the basis of a simple effective-mass model which suffices for a general qualitative picture, but given their evidence and interest it seems advisable to study the basic issues more thoroughly on the basis of a more elaborate model, as will be explained

in section 2.

The purpose of the present work is to make a detailed study of the density of states, spatial localization and transmittance (i) for the same GaAs-based well structures [1, 17] as in figure 1(a), (b) and (ii) for the barrier structures of figure 1(c), (d) and to do it in parallel for the analogue and digital structures in order to compare their properties.

2. The model and method

We study the structures shown in figure 1, involving GaAs and $Al_xGa_{1-x}As$. The well structure is that of reference [1], with a width of 122 monolayers (344 Å). For the analogue case x varies between 0.28 (barrier) and 0 (bottom of the well). The digital structure has alternate values $x = 0.28$ and $x = 0$. The barrier structures, also 344 Å thick, are likewise described.

It has been recognized that the usual effective-mass models are inadequate for providing a reasonably satisfactory account of the electrical and optical properties of multibarrier quantum well structures and one must take into account the complexities of the band structures of the constituent materials more carefully [29]. Although it could be possible to extend the envelope-function approximation to include valley-mixing effects at the interfaces [30–33], it has been seen that the connection rule at the interface is very complicated and changes in the location of the interface within a lattice constant produce appreciable changes in the eigenenergies [34]. Because of this we shall use an empirical tight-binding model, which includes the multiband and band-mixing characteristics together with the crystalline symmetry for the constituent materials. We use the same empirical tight-binding sp^3s^* model previously used and described [14–17] and perform Green function calculations. For the central, inhomogeneously graded or digitally structured region, the Green function is obtained by means of the algorithm developed in [14] and used in [15–17] and this is then matched at the extremes of the 344 Å thick region to the material outside—$x = 0.28$ or $x = 0$—by using surface Green function matching (SGFM) [35]. All of the details are given in references [14–17, 35] and need not be repeated here.

A convenient way to calculate the transmittance is to use the two-probe Büttiker–Landauer formalism in the Green function version [36]. The 122-monolayer heterostructure is matched on both sides to 67 monolayer slabs of homogeneous material, with $x = 0.28$ (well) or $x = 0$ (barrier). The entire system for which the SGFM analysis finally yields the Green function is then 256 monolayers thick, which is large but *finite*. The leads are then connected to the extremes of the entire system. It will be presently seen that its finiteness has some technical consequences.

3. Results for well structures

In the reference frame used here the top of the valence band of AlAs is at $E = 0$ eV, the bottom of the conduction band of GaAs is at $E = 2.10$ eV, that of AlGaAs ($x = 0.28$) is at $E = 2.363$ eV, and all of the calculations were performed for the $\bar{\Gamma}$ point, $\boldsymbol{\kappa} = (0, 0)$. The range of bound states, 2.10 eV $< E <$ 2.36 eV, was studied in [17] and substantial differences in the spatial localization of the higher bound states were found between the analogue (AQW) and digital quantum wells (DQW). Here we study the transmission coefficient T in the energy range of propagating states starting at $E = 2.36$ eV. Figure 2(a) shows $\log T$ as a function of E from 2.36 to 2.50 eV for the AQW, the DQW and also a regular multiquantum well or finite superlattice structure to be discussed later.

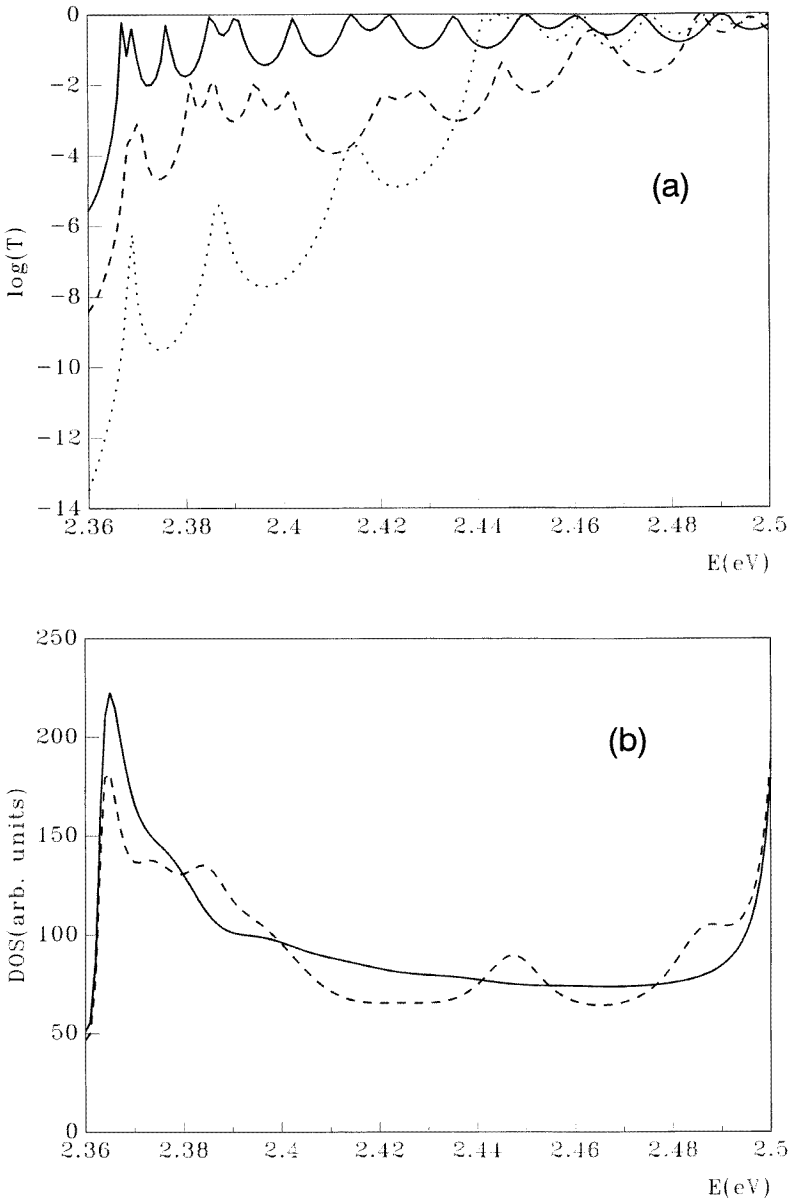

Figure 2. (a) The logarithm of the transmission coefficient T for three different quantum well structures in the energy region just above the barrier. The bottom of the conduction band of AlGaAs ($x = 0.28$) is, in the reference frame used here, at 2.363 eV. Full line: the analogue structure (figure 1(a)). Dashed line: the digital structure (figure 1(b)). Dotted line: the finite superlattice (see the text). (b) The density of states in the same energy region.

The calculation was also carried out for a 256-monolayer-thick slab of homogeneous bulk AlGaAs ($x = 0.28$). Ideally (i.e., for an infinite homogeneous system) the transmittance should be unity in the range of allowed propagating states of the material, but the results—not shown in the figure—show a sequence of dips to lower values, negative in the logarithmic

scale, practically like those seen on the right-hand side of the full curve of figure 2(a). These are merely a consequence of the finite size of the sample, a fact checked by halving or doubling the size. This can be easily done with the SGFM method because it does not change the size of the matrices required. The result of the calculation was that on doubling/halving the size of the sample these dips are shallower/deeper and more densely/sparsely spaced. Thus these oscillations are not intrinsic but merely an artifact of the method employed to calculate the transmittance. The point is that this can be avoided by using fully the SGFM method to calculate the transmittance, but then this would require calculating explicitly the wavefunctions and this does involve substantial extra computation. The Büttiker–Landauer formalism is inherently more suitable for smaller systems, but in the Green function version used here it is a convenient practical device to study with substantial economy of computation the problems raised here while availing ourselves of algorithms and formalisms of proven practical usefulness to describe the total slab containing the heterostructure of interest. Discarding the down oscillations as an artifact due to the finite size of the sample connected to the leads, the essence of the problems considered here can then be studied in a convenient practical way. This observation should be kept in mind in the discussion of all the results shown here for the transmittance.

Returning now to the results obtained for the AQW (the full line in figure 2(a)) there is first a very narrow energy range just above the barrier where the effect of the well is to produce a very low transmittance, after which T exhibits a quasiregular behaviour which soon becomes quite regular and very similar to that obtained for the homogeneous barrier material. For the reasons just explained this means that T is high, essentially unity, for $E \geqslant 2.4$ eV. The DQW (dashed line) is in this respect substantially different. Starting from the barrier level, T is more than one order of magnitude smaller, which amounts in practice to a transmittance gap of about 0.1 eV. The same observation concerning the finite size of the sample holds here, but the DQW has maxima at distinctly different positions. The difference is also apparent in the density of states (DOS, figure 2(b)) in this energy range. For the AQW this is smooth and very similar to that of the homogeneous bulk material except that the characteristic band-edge singularity is slightly displaced and rounded off to a sharp peak which continues smoothly the very narrow initial energy range in correspondence with the very low T-range of figure 2(a), just above the barrier level. The DOS for the DQW (the dashed line) has a similar overall behaviour but with significant differences of detail, such as the humps at 2.387, 2.445 and 2.486 eV, reflected in corresponding peaks in figure 2(a). The nature of these features can be understood by selecting some representative cases and studying the spatial distribution of the spectral strength of the corresponding states as shown in figure 3.

Case (a) is the AQW, with $E = 2.447$ eV. This has significant amplitude across the well and is therefore a state of high transmittance, as seen in figure 2(a). Its amplitude is somewhat depleted in the well region, a qualitative feature also found in the range of propagating states for rectangular single or double quantum wells [19] and for separate confinement heterostructures [20]. This brings into the picture a feature which will be further discussed later. With rectangular composition profiles what one has in real space is adjacent planar slabs of different materials and this tends to cause *some* diffraction, depending on the details of the heterostructure. In the systems just mentioned [19, 20] it is possible to find an increase in the transmittance at some energies where a resonance with the continuum appears, with some accumulation of amplitude which denotes some constructive interference. This is not found at any energy in our calculation for the AQW, where the asymmetric linear profile breaks any possible coherence needed for constructive interference.

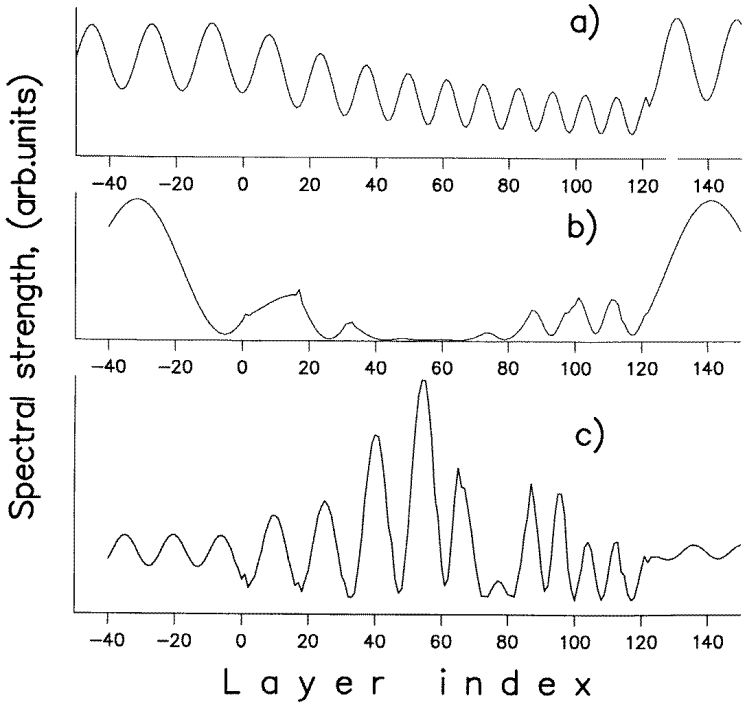

Figure 3. The spatial distribution of the spectral strength (the local density of states) for three states selected from figure 1: (a) the AQW, $E = 2.447$ eV; (b) the DQW, $E = 2.373$ eV; (c) the DQW, $E = 2.488$ eV. The position is given as the layer number on the abscissae. The well region is between layers 0 and 122.

Case (b) is the DQW, with $E = 2.373$ eV. This is a state of very low transmittance (figure 2(a)) not masked by any size effects. The digital structure is a rectangular sequence, and in this case it is capable of producing considerable destructive interference, resulting in a domain inside the well region where the amplitude is practically nil, corresponding to a very low transmittance. The opposite behaviour is illustrated by curve (c), also for the DQW but for $E = 2.488$ eV. This is a state of high transmittance for which constructive interference results in an accumulation of amplitude in the well region. Transmittance gaps at energies above the barriers have been reported for some multiple-quantum-well structures and for finite superlattices formed by a finite sequence of identical wells and barriers [23–27], due to quantum interference effects. Bragg reflectors and Fabry–Perot electron filters based on these effects are actually used in practice [25–27]. In order to see how this relates to the present calculations for the AQW and the asymmetric DQW we have studied a finite superlattice consisting of eight equal quantum wells, seven monolayers wide and seven equal barriers, nine monolayers wide. This has a total thickness of 119 monolayers, very close to the 122 monolayers of the DQW, with which it is to be compared. The regular structure in this case causes strong destructive interference resulting in very low transmittance up to $E \cong 2.44$ eV (figure 2(a), the dotted curve), after which T tends to behave practically like in the homogeneous barrier material. Thus for the initial energy range the regular multiwell structure exhibits stronger interference effects than the asymmetric DQW, which in turn is capable of producing comparatively stronger interference than the 'equivalent' AQW.

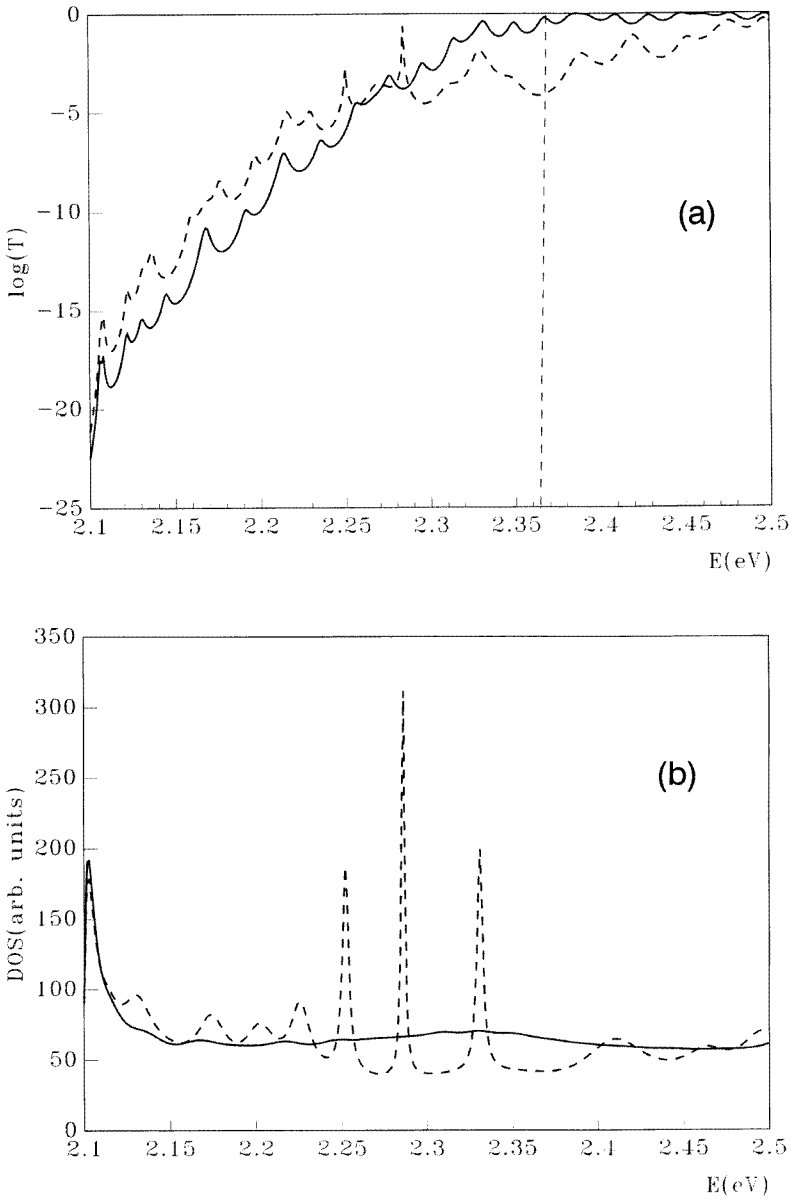

Figure 4. (a) The logarithm of the transmission coefficient T for the barrier structures of figure 1. Full line: the analogue quantum barrier (the AQB; figure 1(c)). Dashed line: the 'equivalent' digital quantum barrier structure (the DQB; figure 1(d)). (b) The density of states for the same systems. Energies span the range from 2.10 eV (the bottom of the GaAs conduction band) to 2.50 eV, above the barrier, i.e. the bottom of the AlGaAs ($x = 0.28$) conduction band at $E = 2.363$ eV, indicated by a vertical line in the figure (in (a) only).

4. Results for barrier structures

Figure 4(a) gives $\log T$ versus E for the analogue (AQB) and digital (DQB) structures of figure 1(c) and 1(d), respectively, spanning an energy range from the bottom of the GaAs

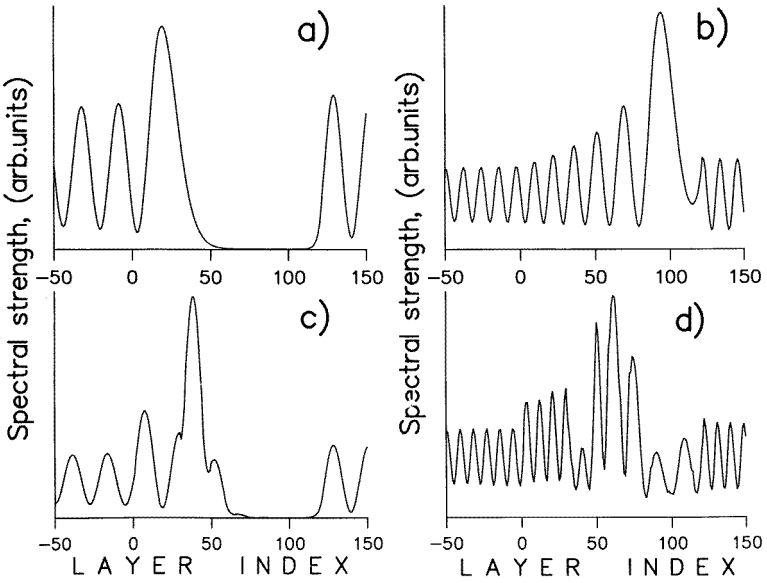

Figure 5. Local spectral strengths for four states selected from figure 4: (a) the AQB, $E = 2.167$ eV; (b) the AQB, $E = 2.331$ eV; (c) the DQB, $E = 2.176$ eV; (d) the DQB, $E = 2.466$ eV.

conduction band to above the barrier level, i.e. the bottom of the AlGaAs ($x = 0.28$) conduction band, indicated by a vertical line in the figure. The results look like what one would expect. The AQB has a very low transmittance at first until above about $E = 2.33$ eV, close to the tip of the triangular barrier, it starts to behave like the bulk GaAs material, results again not shown in the figure but subject to the same general comments as in section 3. The DQB has a larger opacity range, essentially up to $E \cong 2.47$ eV, above the barriers. There is a notable exception at $E = 2.286$ eV, where T is close to unity, which can be understood from the behaviour of the DOS (figure 4(b)). At this energy the digital structure has a sharp high peak denoting a very strong resonance. However, the scrutiny of the spatial distribution of the spectral strength of some selected states (figure 5) shows an unexpected feature for the AQB case. In the low-transmittance range (figure 4(a)) one finds what is to be expected. The barrier repels the amplitude because the energy is still too far below the tip of the triangular barrier and the transmittance is very low. But at the onset of the high-T range, for $E = 2.331$ eV, close to but below the barrier tip at 2.363 eV, the analogue triangular barrier exhibits a substantial accumulation of amplitude at about the spatial location where the barrier height locally equals 2.33 eV. There is no peak in the DOS curve (figure 4(b), full line) at or near this energy and one would not expect constructive interference from the asymmetric triangular profile for the same reasons as in the case of well structures, so this is probably a consequence of the complexity of the model employed to describe the band structure of the materials involved. In this model each state is a combination of different orbital components and it is possible that, besides the diffraction caused by digital structures, the refraction caused by analogue profiles may affect differently the different orbital components, thus producing in some cases effects which, as in the case of figure 5(b) for a triangular barrier, would not appear in a simple one-band model.

The case of the DQB is clear. For $E = 2.466$ eV, where the range of high T roughly starts, there is an accumulation of amplitude (figure 5(d)) which, for the digital structure can be interpreted as the result of some constructive interference. Alternatively, one can take the view that a digital structure, whether of a barrier type or well type, always involves a sequence of wells and one of these may dominate the situation at some energy where by itself it would tend to trap a bound state. This, which was demonstrated in previous calculations [17], is borne out by the results shown in figure 6.

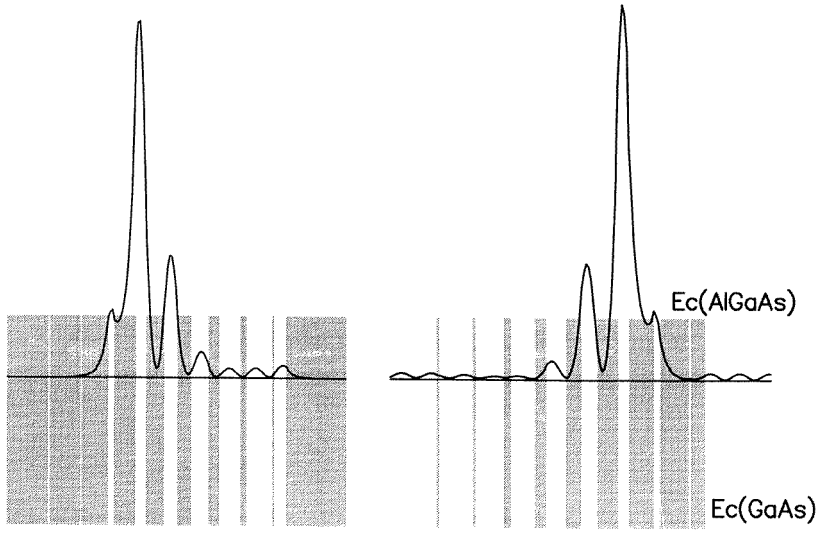

Figure 6. Left-hand side: the DQW of figure 2(b). Right-hand side: the DQB of figure 2(d). The figure gives the spatial distribution of the spectral strength of the state obtained at $E = 2.286$ eV, which is a bound state for the DQW and a (strong) resonance for the DQB. To help visualize the situation, the composition profiles of figure 2 are here replaced by the profile of the conduction band bottom (E_c) across the structure. The horizontal line then situates the energy level under study relative to E_c.

The DQW and DQB are the 'negative' of each other, as one of the structures is obtained from the other one by replacing wells/barriers by barriers/wells. At $E = 2.286$ eV the DQB has a high transmittance—the sharp peak in figure 4(a)—corresponding to the strong resonance seen in figure 6(b). At the same energy the DQW has an actual bound state (figure 6(a)) caused by the same well that attracts the same state in the DQB. The only difference is that in this case this energy resonates with the continuum of propagating states in GaAs, resulting in a sharp peak in the transmittance, but both structures exhibit the same bound state due to the same well, which bears out the nature of the digital structures.

5. Conclusions

Firstly we note that while simple one-band models may have some limited usefulness for comparatively simple structures involving rectangular wells, they may not be reliable in many cases, especially in analogue structures with inhomogeneous composition profiles. A good example is the result shown in figure 5(b). But the same holds for the digital structures, which also involve rectangular wells but in a more complicated way. We have performed

some parallel calculations with effective-mass one-band models and found, among other results, the following, for instance.

(i) For the DQW the transmittance gap of about 0.1 eV just above the conduction band bottom of AlGaAs ($x = 0.28$) seen in figure 2(a) does not appear in the one-band calculation. The low-T region is then only a very narrow energy range of order 0.01 eV, like in the AQW and for the same reasons. Thus in the one-band model the analogue and digital structures have very similar properties and the calculation fails to reveal some features associated with the fact that the latter, although to a lesser extent than the more regular structures, is able to produce some diffraction effects.

(ii) The tight-binding study of the AQW versus the DQW shows that while the eigenvalues of the bound states may be very similar, the spatial distribution of their spectral strengths may be quite different. In contrast, in the one-band calculation they turn out to be very similar. The lesson is that simple models may miss out some distinctive features which differentiate the (refractive) analogue structures from the (diffractive) digital ones.

What basically characterizes the digital structures is that, while not regular, they are to some extent diffractive and can therefore exhibit some quantum mechanical interference effects, though not sharp ones. If one studies a rather more regular structure, like the multiquantum well or finite superlattice of figure 2(a) (the dotted line), then these effects are stronger by orders of magnitude. The extreme case is the full superlattice, where quantum mechanical interference is fully destructive at the precise wavelengths where Bragg reflection takes place, and minigaps appear. Electron interferometry is based on just this fact in smaller but fully regular heterostructures designed to this effect. Interference is then sharp and takes place at a well defined wavelength. In DQW or DQB heterostructures it is not sharp, but there are some ranges of wavelengths, determined by the design parameters, where it is stronger. This explains their distinctive differences of detail with respect to their 'equivalent' analogue structures and shows the limitations of the supposed 'equivalence'.

Acknowledgments

AA is especially indebted to the Spanish Ministry of Education and Science for support. SV is especially indebted to NATO for support. GM is especially indebted to the European Community for support. This work was partially supported by the Spanish DGICYT under Grant No PB93-1251, the European Community through contract No CI1*-CT93-0225 and by NATO under Grant No OUTR.CRG 951371.

References

[1] Pötz W and Ferry D K 1985 *Phys. Rev.* B **32** 3863
[2] Schwartz C 1988 *IEEE J. Quantum Electron.* **24** 1712
[3] Giugni St, Tansley T L and Griffiths G J 1991 *J. Cryst. Growth* **111** 50
[4] Giugni St, Tansley T L, Green F, Shwe C and Gal M 1992 *J. Appl. Phys.* **71** 3486
[5] Kopf R F, Herman M H, Schnoes M L and Colvard C 1993 *J. Vac. Sci. Technol.* B **11** 813
[6] Mathine D L, Maracas G N, Gerber D S, Droopad R, Graham R J and McCartney M R 1994 *J. Appl. Phys.* **75** 4551
[7] Lin F C, Chi W S, Huang Y S, Qiang H, Pollak F H, Mathine D L and Maracas G N 1995 *Semicond. Sci. Technol.* **10** 1009
[8] Capasso F, Cox H M, Hutchinson A L, Olsson N A and Hummel S G 1984 *Appl. Phys. Lett.* **45** 1193
[9] Harbison J P, Peterson L D and Leukoff J 1987 *J. Cryst. Growth* **81** 34
[10] Giugni St and Tansley T L 1991 *J. Vac. Sci. Technol.* B **9** 2805
[11] Gossard A C, Miller R C and Wiegmann W 1986 *Surf. Sci.* **174** 131

[12] Sundaram M, Wixforth A, Geels R S, Gossard A C and English J H 1991 *J. Vac. Sci. Technol.* B **9** 1524
[13] Schulman J N 1983 *J. Vac. Sci. Technol.* B **1** 644
Schulman J N and Chang Y Ch 1983 *Phys. Rev.* B **27** 2346
[14] Vlaev S, Velasco V R and García-Moliner F 1994 *Phys. Rev.* B **49** 11 222
[15] Vlaev S, Velasco V R and García-Moliner F 1994 *Phys. Rev.* B **50** 4577
[16] Vlaev S, Velasco V R and García-Moliner F 1995 *Phys. Rev.* B **51** 7321
[17] Vlaev S, Velasco V R and García-Moliner F 1995 *Phys. Rev.* B **52** 13 784
[18] Osbourn G C and Smith D L 1979 *J. Vac. Sci. Technol.* **16** 1529
Osbourn G C 1980 *J. Vac. Sci. Technol.* **17** 1104
[19] Bastard G, Ziemelis U O, Delalande C, Voos M, Gossard A C and Wiegmann W 1984 *Solid State Commun.* **49** 671
[20] Bastard G 1984 *Phys. Rev.* B **30** 3547
[21] Colocci M, Martínez-Pastor J and Gurioli M 1993 *Phys. Rev.* B **48** 8089
[22] Dossa D, Lew Yan Voon L C and Ram-Moham L R 1991 *Appl. Phys. Lett.* **59** 2706
[23] Lipsanen H K, Taskinen K and Airaksinen V M 1995 *Solid State Commun.* **93** 525
[24] Capasso F, Sirtori C, Faist J, Sirco D L, Sung-Nee Chu G and Cho A Y 1992 *Nature* **358** 565
[25] Lenz G and Salzman J 1990 *Appl. Phys. Lett.* **56** 871
[26] Zahler M, Brener I, Lenz G, Salzman J, Cohen E and Pfeiffer L 1992 *Appl. Phys. Lett.* **61** 949
[27] Sirtori C, Capasso F, Faist J, Sirco D L, Sung-Nee Chu G and Cho A Y 1992 *Appl. Phys. Lett.* **61** 898
[28] Fujiwara A, Takahashi Y, Fukatsu S, Shiraki Y and Ito R 1995 *Phys. Rev.* B **51** 2291
[29] Taniyama H and Yoshii A 1996 *Phys. Rev.* B **53** 9993
[30] Ando T, Wakahara S and Akera H 1989 *Phys. Rev.* B **40** 11 609
[31] Ando T and Akera H 1989 *Phys. Rev.* B **40** 11 619
[32] Ando T 1993 *Phys. Rev.* B **47** 9621
[33] Einevoll G T and Sham L J 1994 *Phys. Rev.* B **49** 10 533
[34] Li T L and Kuhn K J 1994 *Phys. Rev.* B **49** 2608
[35] García-Moliner F and Velasco V R 1992 *Theory of Single and Multiple Interfaces* (Singapore: World Scientific)
[36] Baranger H U and Stone D A 1989 *Phys. Rev.* B **40** 8169